Phototrophic pigment diversity and picophytoplankton in permafrost thaw lakes

A. Przytulska[1,2], J. Comte[1,2,3], S. Crevecoeur[1,2,3], C. Lovejoy[1,2,3], I. Laurion[4] and W. F. Vincent[1,2]

[1]Centre d'études nordiques (CEN) and Département de biologie, Université Laval, Québec City, QC G1V 0A6, CANADA

[2]Takuvik Joint International Laboratory, Centre National de la Recherche Scientifique (France, CNRS UMI 3376) and Département de Biologie, Université Laval, Québec City, QC G1V 0A6, CANADA.

[3]Institut de Biologie Intégrative et des Systèmes (IBIS), Université Laval, Québec City, QC G1V 0A6, CANADA.

[4]Centre d'études nordiques (CEN) and Centre Eau Terre Environnement, Institut national de la recherche scientifique (INRS-ETE), Québec City, QC G1K 9A9, CANADA

Running title: Phototrophs in subarctic thaw lakes

Keywords: lakes; permafrost; phytoplankton; picocyanobacteria; picoeukaryotes; autotrophic picoplankton; pigments; protists; thermokarst

Biogeosciences special issue: 'Freshwater ecosystems in changing permafrost landscapes'.

Abstract

Permafrost thaw lakes (thermokarst lakes) are widely distributed across the northern landscape, and are known to be biogeochemically active sites that emit large amounts of carbon to the atmosphere as CH_4 and CO_2. However, the abundance and composition of the photosynthetic communities that consume CO_2 have been little explored in this ecosystem type. In order to identify the major groups of phototrophic organisms and their controlling variables, we sampled 12 permafrost thaw lakes along a permafrost degradation gradient in northern Québec, Canada. Additional samples were taken from 5 rock-basin reference lakes in the region to determine if the thaw lakes differed in limnological properties and phototrophs. Phytoplankton community structure was determined by high performance liquid chromatography analysis of their photoprotective and photosynthetic pigments, and autotrophic picoplankton concentrations were assessed by flow cytometry. One of the black colored lakes located in a landscape of rapidly degrading palsas (permafrost mounds) was selected for high-throughput 18S rRNA sequencing to complement conclusions based on the pigment and cytometry analyses. The results showed that the limnological properties of the thaw lakes differed significantly from the reference lakes, and were more highly stratified. However, both waterbody types contained similarly diverse phytoplankton groups, with dominance of the pigment assemblages by fucoxanthin-containing taxa, as well as chlorophytes, cryptophytes and cyanobacteria. Chlorophyll *a* concentrations (Chl *a*) were correlated with total phosphorus (TP), and both were significantly higher in the thaw lakes (overall means of 3.3 µg Chl *a* L^{-1} and 34 µg TP L^{-1}) relative to the reference lakes (2.0 µg Chl *a* L^{-1} and 8.2 µg TP L^{-1}). Stepwise multiple regression of Chl *a* against the other algal pigments showed that it was largely a function of alloxanthin, fucoxanthin and Chl *b* (R^2 = 0.85). The bottom waters of two of the thaw lakes also contained high concentrations of bacteriochlorophyll *d*, showing the presence of green photosynthetic

sulphur bacteria. The molecular analyses indicated a relatively minor contribution of diatoms, while chrysophytes, dinoflagellates and chlorophytes were well represented; the heterotrophic eukaryote fraction was dominated by numerous ciliate taxa, and also included Heliozoa, Rhizaria, chytrids and flagellates. Autotrophic picoplankton occurred in biovolume concentrations up to 3.1×10^5 μm^3 mL^{-1} (picocyanobacteria) and 1.9×10^6 μm^3 mL^{-1} (picoeukaryotes), and varied greatly among lakes. Both groups of picophytoplankton were positively correlated with total phytoplankton abundance, as measured by Chl *a*; picocyanobacteria were inversely correlated with dissolved organic carbon, while picoeukaryotes were inversely correlated with conductivity. Despite their net heterotrophic character, subarctic thaw lakes are rich habitats for diverse phototrophic communities.

1 Introduction

Degradation of ice-rich permafrost leads to the formation of thaw lakes, which are among the most abundant aquatic habitats in high latitude regions (Pienitz et al., 2008; Jones et al., 2012). These environments have attracted increasing scientific interest because of their biogeochemical reactivity. However, although there is rapidly increasing knowledge about their role in greenhouse gas (GHG) emissions (Laurion et al., 2010; Walter et al., 2006), little is known about their photosynthetic communities. Phototrophic organisms consume CO_2 and thereby reduce the net emission to the atmosphere; however, few studies have examined phytoplankton or other phototrophs in these abundant waters. Early studies in the U.S. Tundra Biome Program at Barrow, Alaska, recorded 105 species of algae in tundra lakes and ponds, with dominance of cryptophytes and chrysophytes (Alexander et al., 1980). More recent studies have focused on thaw lake diatoms as paleolimnological indicators, but the dominants in these records are often benthic taxa such as *Pinnularia* and *Fragilaria* (Bouchard et al., 2013). A lake survey in the western Hudson Bay lowlands, including in permafrost catchments, showed that the phytoplankton had diverse communities, primarily composed of cyanobacteria, chrysophytes, chlorophytes, cryptophytes, dinoflagellates and diatoms (Paterson et al., 2014).

Picophytoplankton (PP), consisting of picocyanobacteria and picoeukaryotes (nominally defined as cells 1 to 3 μm in diameter), contribute a major fraction of the total phototrophic biomass across a wide range of aquatic ecosystems (Richardson and Jackson, 2007), including northern lakes and rivers (Waleron et al., 2007; Vallières et al., 2008). In subarctic (Bergeron and Vincent, 1997) and high arctic (van Hove et al., 2008) lakes, picocyanobacteria may dominate the phytoplankton community in terms of biomass as well as cell abundance. For example, in

77 large oligotrophic Clear Water Lake (Lac à l'Eau Claire, Nunavik, Canada), small cell
78 phytoplankton (cell fraction that passed through a 2 μm filter) accounted for 75% of the total
79 phytoplankton Chl *a* (Bergeron and Vincent, 1997). However, the suitability of permafrost thaw
80 lakes as a habitat for picophytoplankton has not been explored.
81
82 Our overall aim in the present study was to evaluate the major groups of phytoplankton in
83 subarctic thaw lakes, and to relate this abundance and community structure to environmental
84 variables. For this we employed phototrophic pigment analysis by high performance liquid
85 chromatography (HPLC), an approach that has been applied with success to describe
86 phytoplankton community structure at the phylum level in a wide range of freshwater (e.g., Fietz
87 and Nicklisch 2004) and marine (e.g., Ansotegui et al., 2001) studies.
88
89 A secondary objective was to determine the abundance and distribution of picocyanobacteria and
90 picoeukaryotes. As a further guide to the composition of the eukaryotic plankton, and in support
91 of the pigment and picoeukaryote observations, we also applied high throughput 18S rRNA
92 sequencing to surface and bottom waters from one selected lake that was strongly influenced by
93 permafrost degradation. Our study included a wide range of small lakes across the gradient of
94 permafrost degradation in Subarctic Quebec, Canada, from sporadic permafrost landscapes in the
95 south (less than 10% of the area containing permafrost) to discontinuous permafrost in the north
96 (10-90% permafrost). We also took comparative samples from a set of shallow rock-basin lakes
97 that are unaffected by thermokarst processes. Given their limnological variability, as indicated by
98 the variety of water colors among thaw lakes, we hypothesized that there would be large
99 variations in total phytoplankton pigment concentration, pigment diversity and

100 picophytoplankton biovolume. Degrading permafrost soils release dissolved organic carbon
101 (DOC) and fine inorganic particles into the thaw lakes, and these constituents determine the
102 attenuation of light down the water column and the variability in color (Watanabe et al., 2011).
103 DOC also influences the near surface thermal and stratification regime (Caplanne and Laurion,
104 2008), and temperature is known to exert a direct effect on phytoplankton community structure,
105 particularly favouring cyanobacterial dominance (Paerl and Huisman, 2008). We therefore
106 hypothesised that DOC and temperature would be the primary drivers of variations in
107 phytoplankton pigmentation and picophytoplankton biovolume.
108

109 **2 Materials and Methods**

110 **2.1 Study Sites**

111 Twelve thaw lakes (small perennial waterbodies created by thermokarst erosion of the
112 permafrost) were sampled in subarctic Québec during the period of warm open-water conditions,
113 in August 2011 and 2012 (Table S1). The lakes were distributed along a north-south permafrost
114 degradation gradient and across four geographically distinct locations: the Sasapimakwananisikw
115 River valley (SAS) and the Kwakwatanikapistikw River valley (KWK) near Whapmagoostui-
116 Kuujjuarapik; and the Sheldrake River valley (BGR) and the Nastapoka River valley (NAS) near
117 Umiujaq. The KWK and SAS valleys occur within the sporadic permafrost landscape, while the
118 BGR and NAS valleys are located in the discontinuous permafrost landscape (Fig. 1). Each
119 valley is characterised by distinct vegetation cover and soil structure. Lakes located within the
120 KWK valley are situated on impermeable clay-silt beds where the drainage basin is covered with
121 dense shrub vegetation (Breton et al., 2009), whereas lakes in the SAS valley are located in
122 peatlands in which permafrost mounds (palsas) are thawing and degrading rapidly (Bhiry et al.,

123 2011). The lakes located in the northern valleys (BGR, NAS) are situated on marine clay-silt
124 beds and are surrounded by forest and shrub tundra. In addition to twelve permafrost thaw lakes,
125 a set of five shallow rock-basin lakes (SRB) located on basalt bedrock was sampled in the
126 vicinity of Whapmagoostui-Kuujjuarapik. These provided a set of reference lakes that are
127 located at the same latitude and climatic setting, but without the direct influence of degrading
128 permafrost that is experienced by the thaw lakes. The dates of sampling are given in Table S1.
129

130 **2.2 Physicochemical analyses**

131 Profiles of temperature, dissolved oxygen, conductivity, and pH of the 17 lakes were recorded
132 with a 600R multiparametric probe (Yellow Springs Instrument Co.). Additionally temperature
133 and conductivity were recorded with RBR XR620 conductivity-temperature-depth profiler
134 (Richard Brancker Research Ltd). Near surface water samples (0.2 m depth) were collected into
135 dark polyethylene bottles, previously washed with 10% hydrochloric acid and rinsed in MQ
136 water. The samples were stored in coolers and transported to laboratory within 4 h of collection.
137 The total nitrogen (TN) and total phosphorus (TP) measurements were performed on unfiltered
138 water samples collected in 125ml bottles, acidified with sulfuric acid (0.2% final concentration),
139 and stored at 4°C until persulfate digestion. TN concentrations were then measured with a Lachat
140 flow injection analyzer and TP concentrations were measured using a Genesys 10UV
141 spectrophotometer (Thermo Spectronic) and standard techniques (Stainton et al., 1977). Total
142 suspended solids (TSS) were collected onto pre-combusted and pre-weighed glass fiber filters
143 (Advantec MFS) that were dried for 2 h at 60°C and weighed on a Sartorius high precision
144 balance. Dissolved organic carbon (DOC), colored dissolved organic matter (CDOM), soluble
145 reactive phosphorus (SRP) and nitrate (NO_3^-) measurements were performed on water filtered

146 through 0.2 μm cellulose acetate filters (Advantec MFS). Samples for DOC analyses were stored
147 in 45 mL dark glass bottles that had been previously burned at 450°C for 4 h and rinsed with MQ
148 water to remove any traces of organic substances. The DOC analysis was with a Shimadzu TOC-
149 5000A carbon analyzer calibrated with potassium biphthalate. CDOM was determined by
150 spectrophotometric absorbance of the filtrates at 320 nm, blanked against filtered MQ water and
151 converted to absorption values. SRP and NO_3^- were measured in the filtrates using standard
152 colorimetric methods (Stainton et al., 1977), and major ions were measured using Dionex ICS
153 2000 ion chromatograph.
154

155 **2.3 Pigment analysis**

156 Near surface (0.2 m depth) and near-bottom water samples (0.2 m above sediments; 50-500 mL)
157 from each lake were filtered onto 25-mm diameter GF/F glass-fibre filters, and immediately
158 frozen and stored at -80°C until pigment extraction in methanol. Pigments were analyzed by high
159 performance liquid chromatography (HPLC) following the protocols and standards described in
160 Bonilla et al. (2005). For some of the statistical analyses, two groups of algal accessory pigments
161 were separated as in Bonilla (2005): photoprotective pigments (canthaxanthin, diadinoxanthin,
162 echinenone, lutein, violaxanthin and zeaxanthin) and light harvesting, photosynthetic pigments
163 (alloxanthin, Chl *b*, fucoxanthin and peridinin). Standards for identification and quantification of
164 pigments (Chl *a*, Chl *b*, Chl *c2*, alloxanthin, β,β-carotene, canthaxanthin, crocoxanthin,
165 diadinoxanthin, echinenone, fucoxanthin, lutein, peridinin, violaxanthin, and zeaxanthin) were
166 obtained from Sigma Inc. (St. Louis, MO, USA) and DHI Water & Environment (Hørsholm,
167 Denmark) to calibrate the HPLC. The photodiode array spectrum of each peak was checked
168 against the reference spectra in Roy et al. (2011). No standards were available for

169 bacteriochlorophyll *d* and the primary peaks for this pigment at 428 nm were expressed as Chl *a*
170 equivalent concentrations.
171
172 **2.4 Picophytoplankton enumeration**
173 Near surface (0.2 m depth), unfiltered water samples from each lake were transferred to 5mL
174 Cryovials, fixed with glutaraldehyde (10% final concentration) and stored at -80°C until analysis
175 for picophytoplankton abundance. The cells were enumerated using a Becton Dickinson flow
176 cytometer (BD FacsCalibur), equipped with an argon laser. Analyses were done at the lowest
177 flow rate (12 µL min^{-1}), using a solution of 1-µm diameter, yellow-green microspheres
178 (Polysciences, Inc) as an internal standard. Bead concentrations in the calibration solution were
179 controlled using TrueCountAbsolute counting tubes (BD biosciences). Picocyanobacteria and
180 picoeukaryotes were distinguished based on their chlorophyll and phycoerythrin fluorescence.
181 Detection of the two groups was performed by the comparison of flow cytograms where cells
182 were discriminated based on their side scatter signals (SSC) and both red (FL3) and orange
183 fluorescence (FL2) as well as FL3 versus FL2. Given the low oxygen conditions observed in the
184 bottom layers of the thaw lakes, samples were also analysed for green sulfur bacteria (FL3 vs
185 SCC). The cytograms were analyzed using the Cell Quest Pro software, with manual gating to
186 discriminate the different populations. For the picophytoplankton biovolume estimates, the
187 diameters of 20 cells of each group in a sample from thaw lake KWK12 were measured under
188 epifluorescence microscopy at 1000x magnification, and were then converted to spherical
189 biovolumes. The measured cell diameters (±SD) were 1.0 ± 0.2 µm for picocyanobacteria and
190 2.0 ± 0.5 µm for picoeukaryotes, giving biovolumes per cell of 0.52 and 4.19 μm^3, respectively.
191

192 **2.5 RNA sampling and analysis**

193 Water samples from the near surface (0.2 m depth) and near-bottom (0.2 m above sediments) of
194 the black palsa lake SAS2A were first prefiltered through a 20 µm mesh to remove larger
195 organisms and then filtered sequentially through a 3 µm pore size, 47 mm diameter
196 polycarbonate filter (DHI) and a 0.2 µm Sterivex unit (Millipore) with a peristaltic pump. From
197 100 to 300 mL of water were filtered and the filtration was stopped after 2 hours to minimize
198 RNA degradation. The 3 µm filter for larger cells (L fraction) and the 0.2 µm filter for the
199 smaller fraction (S fraction) were both preserved in RNAlater (Life Technologies) and then
200 stored at -80°C until extraction.
201
202 Samples were extracted with the AllPrep DNA/RNA Mini Kit (Qiagen). This protocol was
203 modified by the addition of cross-linked polyvinylpyrrolidone (PVP, Alfa Aesar) (UV light
204 sterilized) to a final concentration of 10% before loading the samples onto the lysate
205 homogenization column. For all samples, the extracted RNA was converted to cDNA
206 immediately with the High Capacity cDNA Reverse Transcription Kit (Applied Biosystems-
207 Ambion) and stored at -80°C until analysis. The V4 region of the eukaryotic 18S rRNA that had
208 been converted to cDNA was amplified using the 454 primers as described in Comeau et al.
209 (2011). PCR was carried out in a total volume of 50 µL, the mixture contained HF buffer 1X
210 (NEB), 0.25 µM of each primer, 200 µM of each dNTPs (Life Technology), 0.4 mg mL^{-1} BSA
211 (NEB), 1 U of Phusion High-Fidelity DNA polymerase (NEB) and 1 µL of template cDNA. Two
212 more reactions with 5X and 10X diluted template were also carried out for each sample, to
213 minimize potential primer bias. Thermal cycling began with an initial denaturation at 98°C for
214 30 s, followed by 30 cycles of denaturation at 98°C for 10 s, annealing at 55°C for 30 s,

extension at 72°C for 30 s and a final extension at 72°C for 270 s. The three dilution reactions were pooled and purified with a magnetic bead kit Agencourt AMPure XP (Beckman Coulter) and then quantified spectrophotometerically with the Nanodrop 1000 (Thermo Fisher Scientific). The amplicons were sequenced on 1/8 plates of the Roche 454 GS-FLX using the "PLUS" chemistry at the IBIS/Laval University, plate-forme d'analyses Génomiques (Québec City, QC). The raw 454 sequences have been deposited in the NCBI database under the bioproject name PRJNA286764.

Sequences were analysed using the UPARSE pipeline (Edgar, 2013). For quality filtering, the sequences were truncated at 245 bp to keep 50% of the reads at the 0.5 expected error rate. Singletons as well as chimeras were then removed and operational taxonomic units (OTUs) were determined at the ≥ 98% similarity level. These OTUs were classified using the mothur classifier (Schloss et al., 2009) with a 0.8 confidence threshold based on the SILVA reference database (Pruesse et al., 2007) modified to include sequences from our in-house, curated northern 18S rRNA gene sequence database. In order to compare samples, the OTU tables were each subsampled 100 times at 2200 reads, which corresponded to the lowest number of reads per sample minus 10%; this subsampling used the command multiple_rarefaction_even_depth.py in Qiime (Caporaso et al., 2010). The most abundant and unclassified OTUs were subsequently submitted to a BLASTn search to the nr database in NCBI GenBank (http://blast.ncbi.nlm.nih.gov/Blast.cgi) to identify the nearest match.

2.6 Statistical analysis

The normal distribution of environmental variables was tested using the Kolmogorov-Smirnov test, and right-skewed variables were normalized by natural logarithm transformation. Given the order of magnitude differences in picophytoplankton abundances and pigment concentrations among samples, the HPLC and flow cytometry data were also normalized by logarithmic transformation. Correlations within and among the phytoplankton, pigment and environmental variables were tested by Pearson correlation analysis, with correction for multi-testing using the false discovery rate procedure as in Benjamini and Hochberg (1995). To investigate the extent to which environmental variables drove the distribution of pigment diversity among the different water bodies, a redundancy analysis (RDA, Legendre and Legendre, 2012) was run. This was based on Bray-Curtis distances for the pigment matrix (db-RDA) and the data were log-transformed prior to analysis. The significance of the model was assessed via 1000 permutations, and the analysis was performed in RStudio (version 0.98.501) using the Vegan package (Oksanen et al., 2015). Stepwise multiple linear regression models were performed using Past 3.04, with secondary cross-correlated variables removed prior to these analysis.

3 Results

3.1 Environmental heterogeneity

The thaw lakes spanned a wide range of environmental conditions, including water color and CDOM, with the latter strongly correlated with DOC ($R = 0.67$, $p < 0.0001$). The highest DOC concentrations (up to 17 mg L^{-1}) and CDOM (up to 117 m^{-1}) were recorded in the SAS lakes (Table 1). These waters were black in color and also had the lowest pH values (6.0 – 6.6). The highest total nutrient concentrations (up to 125 µg TP L^{-1} and 4 mg TN L^{-1}) were recorded

261 in lakes located within the KWK and NAS valleys, and the values were lowest in the shallow
262 rock-basin waters (minima of 1.6 µg TP L^{-1} and 0.1 mg TN L^{-1}). Nitrogen to phosphorus ratios
263 varied greatly among the 17 lakes, from 4 to 131 (g g^{-1}), and total suspended solids were
264 similarly variable, from 1 to 320 mg L^{-1} (Table 1). The NAS valley waters contained especially
265 high concentrations of suspended clay particles, producing an opaque milky appearance. Despite
266 their shallowness and small size, the thaw lakes were highly stratified in terms of temperature
267 and oxygen (Fig. 2), with anoxic bottom waters in the SAS and KWK lakes. Some had
268 pronounced thermal gradients, with temperature differences up to 10°C between the surface and
269 bottom waters. In contrast, the reference lakes showed more homogenous conditions, indicative
270 of mixing (Fig. 2).
271
272 **3.2 Planktonic pigments**
273 Phytoplankton abundance, as measured by Chl *a* concentrations, varied greatly among the
274 waterbodies (Table 1), from 0.4 (SRB1) to 6.8 (KWK6) µg L^{-1} in 2011 and from 0.2 (SRB1) to
275 9.1 (KWK1) µg L^{-1} in 2012. There was also a small but significant difference in Chl *a*
276 concentrations between years, with means of 3.7 and 2.6 µg L^{-1}, respectively (paired t-test,
277 $t = 2.5$, $p = 0.02$). On average, Chl *a* was significantly higher in the thaw lakes than the reference
278 rock-basin waters: the overall means were 3.3 and 2.0 µg Chl *a* L^{-1}, respectively.
279
280 The pigment analyses of the phytoplankton (Table 2) showed that there were diverse
281 communities including fucoxanthin-containing groups (potentially diatoms, chrysophytes and
282 certain dinoflagellates), chlorophytes (Chl *b*, lutein and violaxanthin), cryptophytes
283 (alloxanthin), dinoflagellates (peridinin) and cyanobacteria (zeaxanthin, canthaxanthin,

284 echinenone). The pigments Chl c_1, c_2, c_3 and crocoxanthin were also present, but generally at
285 trace concentrations, and only in certain lakes. The abundance of cyanobacterial populations in
286 KWK, BGR and NAS lakes was indicated by high concentrations of zeaxanthin (e.g., NASH)
287 and echinenone (SRB3). The KWK lakes had high concentrations of zeaxanthin (up to
288 0.7 nmol L^{-1} in KWK23 lake), accompanied by high concentrations of fucoxanthin and green
289 algal pigments (lutein and violaxanthin), as well as high concentrations of diadinoxanthin (e.g.,
290 KWK1). In the SAS lakes, a dominance of dinoflagellates was indicated by high concentrations
291 of peridinin. Echinenone was present in KWK and SRB lakes and high concentrations of
292 violaxanthin were also recorded in BGR lakes. Fucoxanthin-groups were abundant in SRB and
293 SAS as well as in NASH and BGR2. The turbid thaw lakes within the NAS valley had high
294 concentrations of β,β-carotene. Relatively high levels of ancillary photosynthetic pigments were
295 present in NASA and SAS lakes as well as in some waters of shallow rock-basin lakes (Table 2).
296 Photoprotective pigments were relatively more abundant in KWK lakes (notably KWK1 and
297 KWK6) as well as in the SRB waters (violaxanthin), and less abundant in the DOC-rich SAS
298 lakes (Table 2). The bottom waters of the thaw lakes also contained diverse planktonic pigments,
299 including high levels of diadinoxanthin and alloxanthin in KWK lakes, fucoxanthin in BGR2 and
300 Chl *b* in SRB lakes. High levels of bacteriochlorophyll *d* indicating abundant populations of
301 green photosynthetic sulfur bacteria were recorded in the deeper, anoxic waters of KWK lakes
302 (Table 3, Fig. 4).
303
304 For the overall data set, Chl *a* concentrations were significantly correlated with TP ($R = 0.47$;
305 $p = 0.05$), and with TSS ($R = 0.55$; $P = 0.03$), which were themselves strongly correlated
306 ($R^2 = 0.76$; $p < 0.0001$). A forward stepwise linear regression showed that Chl *a* was best

307 described by a combination of the accessory pigments alloxanthin ($p < 0.014$), fucoxanthin
308 ($p < 0.001$) and Chl *b* ($p < 0.001$): ln Chl *a* = 1.774 + 0.161 ln Allo + 0.380 ln Chl *b* + 0.341 ln
309 Fuco ($R^2 = 0.85$; $p < 0.001$).
310
311 Several pigments were highly cross-correlated. These included alloxanthin and lutein ($R = 0.81$,
312 $p < 0.001$) and both pigments with Chl *b* ($R = 0.71$; 0.92, $p < 0.001$). The chlorophyte pigment
313 violoxanthin was also correlated with Chl *b* ($R = 0.60$, $p < 0.001$) and fucoxanthin ($R = 0.58$, $p <$
314 0.001). The fucoxanthin itself was most strongly correlated with diadinoxanthin ($R = 0.77$, $p <$
315 0.001). The cyanobacterial pigments echinenone and canthaxanthin were significantly correlated
316 ($R = 0.57$, $p < 0.001$), but not with zeaxanthin ($p > 0.05$). The summations within the two
317 categories of pigments, photoprotective and photosynthetic, were also positively correlated ($R =$
318 0.63; $p < 0.001$*).* Consistent with the multivariate analyses, the accessory pigments were
319 uncorrelated with individual environmental variables (all corrected p values were > 0.05), with
320 the exception of lutein. This chlorophyte pigment was significantly correlated with TP ($R = 0.53$;
321 $p = 0.01$), but this may simply reflect the strong correlation between lutein and Chl *a* ($R = 0.79$;
322 $p < 0.0001$), which itself correlated with TP.
323
324 The db-RDA model showed a clear separation of the different valleys in terms of phytoplankton
325 pigment composition. These distinct patterns in pigment composition was partially explained by
326 the influence of valley specific environmental variables. In addition, the results from dbRDA
327 reaffirmed the large lake-to-lake heterogeneity in each of the valleys, even among nearby lakes.
328 The first two canonical components; related to TP, DOC and pH; explained 11% of the total

329 variances in pigment composition (Fig. 3). The dbRDA model as a whole explained 16.4% of the
330 variance (R^2 = 0.16, F= 1.71, df = 8, p = 0.012).
331
332 **3.3 Picophytoplankton abundance and biovolume**
333 Picophytoplankton concentrations varied greatly among the lakes (Fig. 5). The
334 picocyanobacterial abundances ranged from 1.8 x 10^3 cells mL^{-1} (SAS1B) to 5.9 x 10^5 cells mL^{-1}
335 (KWK23), equivalent to biovolume concentrations of 9.5 × 10^2 (SAS1B) to 3.1 × 10^5 μm^3 mL^{-1}
336 (KWK23), while the picoeukaryote abundances ranged from 1.35 × 10^2 cells mL^{-1} (SAS2B) to
337 4.6 × 10^5 cells mL^{-1} (KWK1), equivalent to biovolume concentrations of 5.6 × 10^2 (SAS2B) to
338 1.9 × 10^6 μm^3 mL^{-1} (KWK1). In general, the lakes located on marine clays (KWK and BGR)
339 contained the highest cell concentrations and biovolume of total picophytoplankton. The shallow
340 rock-basin (SRB) and peatland lakes (SAS) were apparently less favourable, with
341 picocyanobacterial and picoeukaryote biovolume concentrations below 10^4 μm^3 mL^{-1}.
342 Picoeukaryotes were generally less numerically abundant than picocyanobacteria, but because of
343 their larger cell size, they dominated total picophytoplankton biomass. Picoeukaryotes accounted
344 on average (±SD) for 65 (±28) % of total picophytoplankton biovolume, however there was a
345 wide range among lakes in this contribution, from 8% (SAS2B) to 99% (SAS1A).
346
347 Total picophytoplankton biovolume increased with Chl *a* concentration (R = 0.52; p = 0.03), but
348 this relationship was only significant for the eukaryotic component (R = 0.53; p = 0.02).
349 Picocyanobacteria correlated negatively with DOC (R = -0.47; p = 0.05), while picoeukaryotes
350 correlated negatively with conductivity (R = -0.48; p = 0.05). Picocyanobacteria were highly
351 correlated with zeaxanthin (R = 0.72; p = 0.0002), and there was also a significant, albeit less

strong, correlation between picoeukaryotes and zeaxanthin (R = 0.54; p = 0.02). Stepwise multiple linear regression models showed that picophytoplankton (picoeukaryotes, PEuk; picocyanobacteria, PCyan) biovolumes were statistically related to certain limnological variables according to the relationships: PEuk = 14.9 + 2.9 × Chl *a* - 1.7 × TN (R^2 = 0.56, p = 0.001), and PCyan = -2.9 + 4.3 Temp + 1.1 × Chl *a* - 1.1 × TSS + 1.5 × TP - 1.2 × DOC (R^2 = 0.67, p = 0.001).

3.4 Molecular analyses

The 18S rRNA data set from the palsa thaw lake (SAS2A) contained large numbers of rotifer sequences (400 to 1350 reads per sample, all with closest matches to the genus *Ascomorpha*) and these were removed prior to further analysis. This left a total of 3857 and 3128 reads for the surface L (> 3.0 μm) and S (< 3.0 μm) fractions, and 3522 and 2457 reads for the bottom L and S fractions; 84 to 93% of these eukaryotic sequences could be assigned (≥ 98% identity) to phylum in the modified SILVA database. The largest fraction of total reads was attributable to ciliates (up to 33% in the surface waters and 74% in the bottom waters; Table 4), including the genus *Stokesia,* especially in the surface waters, and the genera *Cryptocaryon, Halteria*, *Peniculida* and *Cyclidium*, especially in the bottom waters (Table 5). Among the groups nominally considered as phytoplankton were dinoflagellates, chrysophytes and chlorophytes, with lesser proportions of reads associated with katablepharids, bacillariophytes (diatoms) and cryptophytes (Table 4). Analysis of the dissimilarity distances (Bray-Curtis distance on the sub-sampled dataset) showed that community structure greatly differed with depth (Bray-Curtis dissimilarity index of 0.795 for the large fraction and 0.820 for the small fraction), and to a much lesser extent between large and small fractions (Bray-Curtis dissimilarity index of 0.423 for the surface samples and 0.312

for the bottom samples). Chlorophytes, dinoflagellates, katablepharids and diatoms were more represented in the large, surface water fraction.

4 Discussion

Each of the subarctic thaw lakes contained pigments from several phytoplankton phyla, revealing that these abundant waters provide habitats for diverse phototrophic groups., The most abundant accessory pigment (apart from β,β-carotene present in all algal groups) was fucoxanthin, indicating the possible presence of diatoms, chrysophytes or certain dinoflagellates. Peridinin and alloxanthin were also present in many of the samples, indicating the presence of dinoflagellates and cryptophytes, respectively (Jeffrey et al., 2011). Diatoms would be less favoured in these stratified waters given their relatively high sinking rates, while flagellated taxa including chrysophytes, dinoflagellates and cryptophytes would be able to maintain their position in the euphotic zone. Mixotrophic chrysophytes and dinoflagellates have been observed in many high latitude lakes (Charvet et al., 2012; and references therein), and may be additionally favored by the high biomass concentrations of heterotrophic bacteria that occur in some of these waters (Breton et al., 2009; Roiha et al., 2015). Green algae were also well represented at most sites, indicating that despite the strong light attenuation by CDOM and TSS (Watanabe et al., 2011), there is adequate light availability for obligate phototrophs. Another conspicuous feature of the pigment data was the large variation in pigment characteristics among lakes within the same valley, even between adjacent waterbodies. This large within-valley variation has also been observed in bacterial studies in the region (Crevecoeur et al., 2015; Comte et al., 2015).

397 The concentrations of photoprotective pigments were conspicuously high in NASH relative to
398 photosynthetic pigments (Table 2). This was unexpected given that it contained elevated
399 concentrations of suspended solids, which indicate a low light availability for photosynthesis,
400 and a lack of need for protection against bright light. It is possible, however, that in this lake,
401 cells suspended in the mixed layer are adapted to intermittent exposure to bright light rather than
402 the average water column irradiance. Such conditions have been observed in a turbid estuarine
403 environment, where the phytoplankton were photosynthetically adapted to high near-surface
404 irradiances rather than the overall shade or dark conditions experienced on average by the cells
405 as they were circulated by turbulent mixing through the water column (Vincent et al., 1994). In
406 contrast, the ratio of photosynthetic to photoprotective pigments was high in NASA and the SAS
407 lakes, indicating acclimation to low irradiances in their strongly light-attenuating water columns.
408
409 The pigment analyses also indicated the abundant presence of cyanobacteria. Echinenone and
410 canthaxanthin are well known photoprotective pigments in cyanobacteria, with the latter
411 especially prevalent in Nostocales, which may suggest the presence of nitrogen-fixing taxa.
412 These results are consistent with bacterial 16S rRNA analyses, which showed the presence of
413 cyanobacterial taxa in some of these lakes that had strong affinities (> 99% sequence similarity)
414 to the Nostocalean taxon *Dolichospermum curvum* (Crevecoeur et al., 2015). Zeaxanthin can
415 potentially occur in high cellular concentrations in cyanobacteria, but it also is found in
416 eukaryotic algal groups. This pigment is a component of photoprotective xanthophyll cycles, and
417 may co-occur with other components of these cycles. For example, studies on the diatom
418 *Phaedactylum tricornutum* have shown the co-occurrence of the diadinoxanthin cycle and the
419 violaxanthin cycle (Lohr and Wilhelm 1999). Consistent with this co-occurrence, we found a

420 strong correlation between diadinoxathin and violaxanthin in the studied lakes ($R = 0.72$,
421 $p < 0.001$). We also observed high concentrations of zeaxanthin, which is often associated with
422 cyanobacteria but also chlorophytes (Jeffrey et al., 2011). Given the molecular analyses results of
423 thaw lake bacterial communities (Crevecoeur et al., 2015) and our flow cytometry data,
424 zeaxanthin was likely to at least in part be associated with the abundant picocyanobacteria in the
425 order Synechococcales. The strong correlation between picocyanobacteria and zeaxanthin further
426 supports this relationship.
427
428 HPLC analysis has been used with success in a variety of aquatic ecosystems to not only identify
429 major algal groups, but also to quantify their proportional representation using the software
430 program CHEMTAX (Mackay et al., 1996). However, given the large known variation in
431 pigment ratios in algal cells, this method requires extensive calibration on each class of waters.
432 For example, in shallow a eutrophic lake, CHEMTAX gave a reliable estimation of
433 cyanobacterial and chlorophyte biomass, but not chrysophytes and dinoflagellates (Tamm et al.,
434 2015). The latter were two of the dominant groups in the permafrost thaw lakes, and although
435 CHEMTAX offers a potentially useful approach for future analyses of these waters, further work
436 will be required before it can be calibrated and reliably applied.
437
438 The presence of bacteriochlorophyll *d* in high concentrations in KWK lakes containing anoxic
439 bottom waters indicate that these environments are favourable habitats for photosynthetic sulfur
440 bacteria. These results were unexpected given the strong attenuation of light by the CDOM and
441 suspended particles in these waters, and the low photosynthetically available radiation at depth.
442 However, the results are consistent with molecular analyses of the bacterial assemblages. 16S

443 rRNA gene clone library analysis of KWK lakes detected the presence of green sulfur bacteria
444 (Rossi et al., 2013), and high throughput 16S rRNA sequencing revealed that the green sulfur
445 bacterium *Pelodictyon* (*Chlorobi*) was one of the most abundant sequences in KWK waters
446 (Crevecoeur et al., 2015). The high concentrations of bacteriochlorophyll *d* suggest that these
447 populations could play an important role in the overall primary production of certain thaw lakes,
448 although restricted to deeper water, anoxic conditions, and our observations extend the range of
449 environments in which this pigment has been detected.
450
451 Picophytoplankton occurred in all of the sampled lakes, but with large differences among waters
452 in terms of the relative abundance of prokaryotes versus eukaryotes, and probably also in terms
453 of their contribution to the total phytoplankton community biomass. As a first estimate of the
454 relative contribution of picocyanobacteria, their cell concentrations may be converted to
455 equivalent Chl *a* by an appropriate cell conversion factor. Analysis of *Synechococcus* in culture
456 under different irradiance regimes gave a median value around 7.5 fg Chl *a* per cell (Moore et al.
457 1995), and applying this value as a first order estimate, picocyanobacteria would contribute 0.3%
458 (SAS1B) to 80% (KWK23) of the measured total community Chl *a*. Such estimates are highly
459 approximate given the known variation in the cellular content of this pigment among strains and
460 with growth conditions; for example, by a factor of 4 as a function of irradiance (Moore et al.
461 1995). However these calculations imply large lake-to-lake variations in the percentage
462 contribution of picophytoplankton to the total community, ranging from negligible to major.
463
464 In general, the concentrations of both picocyanobacteria and picoeukaryotes increased with
465 increasing total phytoplankton biomass, as measured by Chl *a* concentrations. However, the two

466 groups differed in their correlative relationships with other limnological variables. In partial
467 support of our initial hypothesis that DOC would be a controlling variable, picocyanobacteria,
468 but not eukaryotes, were negatively correlated with DOC. An inverse relationship with DOC was
469 also found for picophytoplankton in Swedish lakes (Drakare et al., 2003). Similarly in Lake
470 Valkea-Kotinen, in the boreal zone of Finland, variations in autotrophic picoplankton were most
471 closely correlated with water column stability, which in turn was strongly regulated by DOC
472 concentration (Pelromaa and Ojala, 2012). High DOC waters are often characterized by low pH,
473 which may be a constraint on certain cyanobacteria, however acid-tolerant picocyanobacteria are
474 known (Jasser et al., 2013). Even in the low pH SAS waters picocyanobacteria were always
475 present, although in low concentrations (e.g., the minimum of 1.8×10^3 mL^{-1} in SAS2B in 2011).
476 Other factors such as zooplankton grazing may also have played a role in controlling
477 picocyanobacteria (Rautio and Vincent, 2006), although this seems less likely for
478 picocyanobacteria given that they are a nutritionally deficient food source for zooplankton in
479 thaw lakes (Przytulska et al., 2015).
480
481 Picocyanobacteria did not show the expected relationship with temperature in the correlation
482 analyses, although temperature was one of the variables retained in the multiple linear regression
483 analysis. Temperature has often been identified as a key variable for cyanobacterial growth and
484 dominance in lakes elsewhere. For example, in reservoirs in the southeastern USA, there was a
485 strong, positive correlation between picocyanobacterial cell concentrations and temperature,
486 while picoeukaryotes showed an inverse correlation, and dominance of the picophytoplankton
487 community shifted from picoeukaryotes in winter to picocyanobacteria in summer (Ochs and
488 Rhew, 1997). Similarly, increasing temperature favoured picocyanobacteria over picoeukaryotes

489 in German lakes (Hepperle and Krienitz, 2001). In experiments with subarctic lake and river
490 water at 10 and 20°C, the concentration of Chl *a* in the picoplankton fraction increased
491 substantially at the warmer temperature (Rae and Vincent, 1998). The temperature range in the
492 present study may have been too restricted to observe such effects.
493
494 The molecular data provided insight into the large diversity of microbial eukaryotes that occur
495 within the plankton of thaw lake ecosystems, including heterotrophic components such as ciliates
496 and flagellates that may exert grazing pressure on some of the phototrophs. When rotifers were
497 excluded from the analyses, ciliates were dominant in the RNA sequences of SAS2A. This likely
498 reflects not only their cellular abundance but also their large cell sizes with a concomitantly large
499 number of ribosomes; for example, *Stokesia vernalis,* the most abundant sequence identified in
500 the surface waters (Table 5), can be >100 µm in length. Ciliates are also known to be fragile cells
501 that are easily broken up during manipulation like pre-filtration through a 20 µm mesh, which
502 could account for their highly abundant sequences in the S as well as L fractions.
503
504 Chrysophytes and chlorophytes were well represented in the RNA sequences, particularly in the
505 surface water L fraction, consistent with their abundance as indicated by the pigment data.
506 Dinoflagellates constituted the dominant fraction of the phytoplankton sequences, yet were not
507 detected as peridinin in SAS2A, although this pigment was present in two other SAS lakes. This
508 may indicate the presence of large dinoflagellate cells, for example rigid *Ceratium* cells that can
509 extend up to 100 µm in length, but may also be due to the presence of dinoflagellates that lack
510 the accessory pigment peridinin. It should also be noted that the relative abundance of taxa in
511 these analyses may additionally reflect PCR biases in amplification. Diatoms can also include

512 large cell types, but their representation in the sequences was small, suggesting that most of the
513 fucoxanthin that we measured was associated with chrysophytes such as *Uroglena* (Table 5)
514 rather than diatoms. It is of interest that diatoms from the genus *Urosolenia* were the closest
515 match following a BLAST search. This diatom is known to be lightly silicified and may be less
516 susceptible to sedimentation in these well stratified waters. The cryptophyte pigment alloxanthin
517 was in high concentration in SAS2A, as in the other thaw lakes, yet cryptophyte sequences
518 accounted for < 1.5% of the total RNA reads. This might reflect the small cell-size of certain
519 cryptophyte taxa, for example *Chroomonas*.
520
521 The molecular data also provided insight into the nature of the picoeukaryotic communities in
522 the SAS lakes. The taxonomic identities (Table 5) indicated the presence of several chlorophyte
523 genera that are known to produce small cells, notably *Choricystis*, *Lemmermannia*
524 *Monoraphidium* and *Chlorella*. For example, in subalpine Lake Tahoe (USA), *Choricystis*
525 *coccoides* produces cells that are only 0.5 μm^3 in volume, too small to be grazed by calanoid
526 copepods in that lake (Vincent, 1982). Among the chrysophytes, *Spumella* and related genera are
527 known to produce small cells. For all of these analyses, the many unidentified eukaryotic reads
528 add an extra element of uncertainty to the interpretation, but collectively these data underscore
529 the eukaryotic diversity of the thaw lake ecosystem. This parallels the large prokaryotic diversity
530 that has been observed in these lakes, including bacterial phototrophs (Crevecoeur et al. 2015;
531 Comte et al. 2015).
532
533 Permafrost thaw lakes receive large quantities of allochthonous organic carbon from their
534 surrounding catchments and this is reflected in their high DOC and CDOM concentrations, as

observed in the present study. These waters have high respiratory oxygen demands and are net heterotrophic, resulting in prolonged hypoxia or anoxia in the bottom waters during summer, and anoxia throughout the water column once ice covers the lake in winter (Deshpande et al., 2015). The abundant ciliate and nanoflagellate sequences in our molecular analyses also point to high productivity by bacterial heterotrophs, their likely prey in these waters. However, despite these multiple signs of intense heterotrophy, the pigment, cytometry and molecular results in the present study show that these ecosystems are also the habitats for abundant phototrophs from diverse taxonomic groups.

Conclusions

The wide range of thaw lakes sampled in the present study significantly differed from the reference rock basin lakes in their limnological properties. On average, they contained higher phytoplankton (Chl *a*) and TP concentrations than the reference lakes, but had a comparable diversity of pigments, dominated by chlorophyte, chrysophyte and dinoflagellate pigments. Cyanobacteria and cryptophytes were also well represented, but the thaw waters appeared to be less favorable for diatoms, at least during the highly stratified late-summer period. Picophytoplankton occurred in all of the thaw lakes, in some of the waters at high biovolume up to 10^6 μm^3 mL^{-1}, but the proportion of eukaryotes and prokaryotes and their contribution to total phytoplankton biomass varied greatly among the lakes. Molecular analysis of samples from one of a thaw lake originated from a highly degraded permafrost valley indicated that small cell chlorophytes may be among the dominants in the picoeukaryotic fraction. Despite the heterotrophic nature of these organic-rich ecosystems, with respiration likely exceeding photosynthesis throughout the year, permafrost thaw lakes contain abundant, diverse phototrophs

that potentially support higher trophic levels, and that will lessen the net CO_2 release from these waters to the atmosphere.

Author contributions

A. P., W. F. V. and I. L. designed the study; A. P. led the field sampling; S. C. with input from J. C. undertook the molecular analyses under the supervision of C. L.; laboratory analyses were overseen by A. P., W. F. V. and I. L.; flow cytometry analyses were by J. C. and A. P., under the supervision of I. L.; and data analysis was by A. P. with input from J. C., S. C. and W. F. V. A. P. prepared the manuscript with contributions from all co-authors.

Acknowledgments

We thank Marie-Josée Martineau for laboratory assistance with the HPLC analyses, and ADAPT colleagues Paschale Bégin, Bethany Deshpande and Alex Matveev, for assistance in the field. We are also grateful to Maciej Bartosiewicz for his help throughout this project and to Sylvia Bonilla and two anonymous referees for their insightful comments on the manuscript. This study was funded by the Natural Sciences and Engineering Research Council of Canada (NSERC) including the Discovery Frontiers ADAPT grant to W. F. V. and an EnviroNord fellowship to J. C., Fonds de recherche du Québec, the Network of Centres of Excellence ArcticNet and the Canada Research Chair program.

References

Alexander, V., Stanley, D. W., Daley, R. J. and McRoy, C. P.: Primary producers. In: Hobbie, J. E. (ed.) Limnology of tundra ponds, Barrow, Alaska, Dowden, Hutchinson and Ross Inc, Stroudsburg, PA. U.S./IBP synthesis series, 13, 179–250, 1980.

Ansotegui, A., Trigueros, J. M., and Orive, E.: The use of pigment signatures to assess phytoplankton assemblage structure in estuarine waters, Estuarine, Coastal and Shelf Science, 52, 689–703, 2001.

Benjamini, Y., and Hochberg, Y.: Controlling the false discovery rate: a practical and powerful approach to multiple testing, J. R. Stat. Soc., Series B, 57, 289–300, 1995.

Bergeron, M., and Vincent, W. F.: Microbial food web responses to phosphorus and solar UV radiation in a subarctic lake, Aquat. Microb. Ecol., 12, 239–249, 1997.

Bhiry, N., Delwaide, A., Allard, M., Bégin, Y., Filion, L., Lavoie, M., … and Vincent, W. F.: Environmental change in the Great Whale River region, Hudson Bay: Five decades of multidisciplinary research by Centre d'études nordiques (CEN), Ecoscience, 18, 182–203, doi:10.2980/18-3-3469, 2011.

Bonilla, S., Villeneuve, V., and Vincent, W. F.: Benthic and planktonic algal communities in a high arctic lake: pigment structure and contrasting responses to nutrient enrichment, J. Phycol., 41, 1120–1130, doi:10.1111/j.1529-8817.2005.00154.x, 2005.

Bouchard, F., Pienitz, R., Ortiz, JD., Francus, P., and Laurion, I.: Palaeolimnological conditions inferred from fossil diatom assemblages and derivative spectral properties of sediments in thermokarst ponds of subarctic Quebec, Canada, BOREAS 42, 575–595, doi:10.1111/bor.12000, 2013.

Breton, J., Vallières, C., and Laurion, I.: Limnological properties of permafrost thaw ponds in northeastern Canada, Can. J. Fish. Aquat. Sci., 66, 1635–1648, doi:10.1139/F09-108, 2009.

Caplanne, S., and Laurion, I.: Effects of chromophoric dissolved organic matter on epilimnetic stratification in lakes, Aquat. Sci., 70, 123–133, doi:10.1007/s00027-007-7006-0, 2008.

Caporaso, J. G., Kuczynski, J., Stombaugh, J., Bittinger, K., Bushman, F. D., Costello, E. K., and Fierer, N.: Qiime allows analysis of high-throughput community sequencing data, Nat. Methods, 7, 335–336, doi:10.1038/nmeth.f.303.QIIME, 2010.

Charvet, S., Vincent, W. F., and Lovejoy, C.: Chrysophytes and other protists in high Arctic lakes: molecular gene surveys, pigment signatures and microscopy, Polar Biol., 35, 733–748, doi:10.1007/s00300-011-1118-7, 2012.

Comeau, A. M., Li, W. K. W., Tremblay, J. É., Carmack, E. C., and Lovejoy, C.: Arctic Ocean microbial community structure before and after the 2007 record sea ice minimum, PloS ONE, 6, e27492, doi:10.1371/journal.pone.0027492, 2011.

614 Comte, J., Monier, A., Crevecoeur, S. M., Lovejoy, C., and Vincent, W. F.: Bacterial
615 biogeography of permafrost thaw lakes in the changing northern landscape, Ecography, 38,
616 doi: 10.1111/ecog.01667, 2015.

617 Crevecoeur, S., Vincent, W. F., Comte, J., and Lovejoy, C.: Bacterial community structure
618 across environmental gradients in permafrost thaw ponds: Methanotroph-rich ecosystems,
619 Front. Microbiol., 6, 192, doi:10.3389/fmicb.2015.00192, 2015.

620 Deshpande, B. N., MacIntyre S., Matveev A., and Vincent, W. F.: Oxygen dynamics in
621 permafrost thaw lakes: Anaerobic bioreactors in the Canadian subarctic. Limnol. Oceanogr.
622 60: doi:10.1002/lno.10126, 2015.

623 Drakare, S., Blomqvist, P., Bergström, A. K., and Jansson, M.: Relationships between
624 picophytoplankton and environmental variables in lakes along a gradient of water colour and
625 nutrient content, Freshwater Biol., 48, 729–740, doi:10.1046/j.1365-2427.2003.01049.x,
626 2003.

627 Edgar, R. C.: UPARSE: highly accurate OTU sequences from microbial amplicon reads, Nat.
628 Methods,10, 996–998, doi:10.1038/nmeth.2604, 2013.

629 Fietz, S., and Nicklisch, A.: An HPLC analysis of the summer phytoplankton assemblage in
630 Lake Baikal, Freshwater Biol., 49, 332–345, doi: 10.1111/j.1365-2427.2004.01183.x, 2004.

631 Hepperle, D., and Krienitz, L.: Systematics and ecology of chlorophyte picoplankton in German
632 inland waters along a nutrient gradient, Int. Rev. Hydrobiol., 86, 269–284, 2001.

633 Jasser, I., Karnkowska-Ishikawa, A., and Chróst, R. J.: Do acid-tolerant picocyanobacteria exist?
634 A study of two strains isolated from humic lakes in Poland, Hydrobiologia, 707, 209–218,
635 doi:10.1007/s10750-012-1428-y, 2013.

636 Jeffrey, S. W., Wright, S. W., and Zapata, M.: Microalgal classes and their signature pigments.
637 In: Roy, S., Llewellyn, C. A., Skarstad Egeland, E., and Johnsen, G. (eds) Phytoplankton
638 pigments: characterization, chemotaxonomy and aplications in oceanography, Cambridge
639 University Press. (SCOR), 52–53, 2011.

640 Jones, M., Grosse, G., Jones, B. M., and Walter Anthony, K. M.: Peat accumulation in a
641 thermokarst-affected landscape in continuous ice-rich permafrost, Seward Peninsula, Alaska,
642 J. Geophys. Res., 117, G00M07, doi:10.1029/2011JG001766, 2012.

643 Mackey, M. D., Mackey, D. J., Higgins, H. W., and Wright, S. W.: CHEMTAX—a program for
644 estimating class abundances from chemical markers: application to HPLC measurements of
645 phytoplankton, Mar. Ecol.-Prog. Ser., 144, 265–83, doi:10.3354/meps144265, 1996.

646 Moore, L. R., Goericke, R. and Chisholm, S. W.: Comparative physiology of *Synechococcus* and
647 *Prochlorococcus* - influence of light and temperature on growth, pigments, fluorescence and
648 absorptive properties, Marine Ecology Progress Series, 116; 259–275, 1995.

649 Laurion, I., Vincent, W. F., MacIntyre, S., Retamal, L., Dupont, C., Francus, P., and Pienitz, R.:
650 Variability in greenhouse gas emissions from permafrost thaw ponds, Limnol. Oceanogr., 55,
651 115–133, doi:10.4319/lo.2010.55.1.0115, 2010.

652 Legendre, P., and Legendre, L.: Numerical Ecology, 3rd English Edition, Elsevier, 2012.

653 Lohr, M., and Wilhelm, C.: Algae displaying the diadinoxanthin cycle also possess the
654 violaxanthin cycle, Proc. Natl. Acad. Sci. USA, 96, 8784–8789, 1999.

655 Ochs, C. A., and Rhew, K.: Population dynamics of autotrophic picoplankton in a southeastern
656 US reservoir, Int. Rev. Hydrobiol. Hydrogr., 82, 293–313, 1997.

657 Oksanen, J., Blanchet, G. F., Kindt, R., Legendre, P., Minchin, P. R., O'Hara, R. B., Simpson, G.
658 L., Solymos, P., Henry, M., Stevens, H., and Wagner H.: Vegan: Community Ecology
659 Package, R package version 2.2-1, http://CRAN.R-project.org/package=vegan, 2015.

660 Paterson, A. M., Keller, W., Rühland K. M., Jones C. F., and Winter J. G.: An exploratory
661 survey of summer water chemistry and plankton communities in lakes near the Sutton river,
662 Hudson Bay lowlands, Ontario, Canada, Arct. Antarct. Alp. Res., 46, 121–138,
663 doi:10.1657/1938-4246-46.1.121, 2014.

664 Peltomaa, E., and Ojala, A.: Meteorological drivers of the dynamics of autotrophic picoplankton,
665 Freshwater Biol., 57, 1005–1016, doi:10.1111/j.1365-2427.2012.02761.x, 2012.

666 Paerl, H. W., and Huisman, J.: Blooms like it hot, Science, 320, 57–58,
667 doi:10.1126/science.1155398, 2008.

668 Pienitz, R., Doran, P. T., and Lamoureux S. F.: Origin and geomorphology of lakes in the polar
669 regions. Polar lakes and rivers, limnology of Arctic and Antarctic aquatic ecosystems, Oxford
670 University Press, Oxford, UK 25–41, 2008.

671 Pruesse, E., Quast, C., Knittel, K., Fuchs, B. M., Ludwig, W., Peplies, J., … and Glockner, F. O.:
672 SILVA: a comprehensive online resource for quality checked and aligned ribosomal RNA
673 sequence data compatible with ARB, Nucleic Acids Res., 35, 7188–7196,
674 doi:10.1093/nar/gkm864, 2007.

675 Przytulska, A., Bartosiewicz, M., Rautio, M., Dufresne, F., and Vincent, W. F.: Climate effects
676 on high latitude *Daphnia* via food quality and thresholds, PLoS ONE, 10, e0126231,
677 doi:10.1371/journal.pone.0126231, 2015.

678 Rae, R. and Vincent, W. F.: Effects of temperature and ultraviolet radiation on microbial
679 foodweb structure: potential responses to global change, Freshwater Biol., 40, 747–758,
680 doi:10.1046/j.1365-2427.1998.00361.x, 1998.

681 Rautio, M., and Vincent, W. F.: Benthic and pelagic food resources for zooplankton in shallow
682 high latitude lakes and ponds, Freshwater Biol., 51, 1038–1052, doi:10.1111/j.1365-
683 2427.2006.01550.x, 2006.

684 R Core Team R: A language and environment for statistical computing, R Foundation for
685 Statistical Computing, Vienna, Austria, http://www.R-project.org/, 2014.

686 Richardson, T. L., and Jackson, G. A.: Small phytoplankton and carbon export from the surface
687 ocean, Science, 315(5813), 838–840, doi:10.1126/science.1133471, 2007.

688 Roiha, T., Rautio, M., and Laurion I.: Carbon dynamics in highly net heterotrophic subarctic
689 thaw ponds, Biogeosciences, in press, 2015

690 Rossi P., Laurion I., and Lovejoy C.: Distribution and identity of bacteria in subarctic permafrost
691 thaw ponds, Aquat. Microb. Ecol., 69, 231–245, doi:10.3354/ame01634, 2013.

692 Roy, S., Llewellyn, C. A., Egeland, E. S., and Johnsen, G. (Eds.): Phytoplankton pigments:
693 characterization, chemotaxonomy and applications in oceanography, Cambridge University
694 Press., United Kingdom, 845 pp, 2011.

695 Schloss, P. D., Westcott, S. L., Ryabin, T., Hall, J. R., and Hartmann, M.: Introducing mothur:
696 Open-source, platform-independent, community-supported software for describing and
697 comparing microbial communities. Appl. Environ. Microbiol., 75, 7537–7541,
698 doi:10.1128/AEM.01541-09, 2009.

699 Stainton, M., Capel, M., and Armstrong, F.: The chemical analysis of fresh water, 2nd ed.
700 Special Publication 25 Canada Fisheries and Marine Service, 1977.

701 Tamm, M., Freiberg, R., Tõnno, I., Nõges, P., and Nõges ,T.: Pigment-based chemotaxonomy - a
702 quick alternative to determine algal assemblages in large shallow eutrophic lake?, PLoS ONE,
703 10, e0122526, doi:10.1371/journal.pone.0122526, 2015.

704 Vallières, C., Retamal, L., Ramlal, P., Osburn, C. L., and Vincent, W. F.: Bacterial production
705 and microbial food web structure in a large arctic river and the coastal Arctic Ocean,
706 J. Marine Syst., 74, 756–773, doi:10.1016/j.jmarsys.2007.12.002, 2008.

707 Van Hove, P., Vincent, W. F., Galand, P. E., and Wilmotte, A.: Abundance and diversity of
708 picocyanobacteria in high arctic lakes and fjords, Algological Studies, 126, 209–227,
709 doi:10.1127/1864-1318/2008/0126-0209, 2008.

710 Vincent, W. F.: The autecology of an ultraplanktonic shade alga in Lake Tahoe, J. Phycol., 18,
711 226–232, 1982.

712 Vincent, W.F., Bertrand, N., and Frenette, J-J.: Photoadaptation to intermittent light across the
713 St. Lawrence Estuary freshwater-saltwater transition zone, Mar. Ecol.-Prog. Ser., 110, 283–
714 292, 1994.

715 Waleron, M., Waleron, K., Vincent, W. F., and Wilmotte, A.: Allochthonous inputs of riverine
716 picocyanobacteria to coastal waters in the Arctic Ocean, FEMS Microbial. Ecol., 59, 356–
717 365, doi:10.1111/j.1574-6941.2006.00236.x, 2007.

718 Walter, K. M., Zimov, S.A., Chanton, J. P., Verbyla, D., and Chapin, F. S.: III Methane bubbling
719 from Siberian thaw lakes as a positive feedback to climate warming, Nature, 443, 71–75,
720 doi:10.1038/nature05040, 2006.

721 Watanabe, S., Laurion, I., Chokmani, K., Pienitz, R., and Vincent, W. F.: Optical diversity of
722 thaw ponds in discontinuous permafrost: A model system for water color analysis,
723 J. Geophys. Res.-Biogeo., 116, doi:10.1029/2010JG001380, 2011.

724

Table 1. Limnological characteristics including surface values for temperature (T), pH, dissolved organic carbon concentration (DOC), colored dissolved organic matter (CDOM), total suspended solids (TSS), soluble reactive phosphorus (SRP), total phosphorus (TP), total nitrogen (TN), nitrate (NO_3) and Chlorophyll *a* (Chl *a*) in studied subarctic lakes. Mean values from 2011 and 2012 (+/- range in brackets; nd = no data from 2011).

Sites	T (°C)	pH	DOC (mg L^{-1})	CDOM (m^{-1})	TSS (mg L^{-1})	SRP (µg L^{-1})	TP (µg L^{-1})	TN (mg L^{-1})	NO_3 (mg N L^{-1})	Chl *a* (µg L^{-1})
Thaw lakes on marine clays										
BGR1	15.1 (0.7)	7.5 (0.2)	3.9 (0.4)	6.1 (1.7)	2.9 (0.5)	1.8 (0.6)	17.3 (3.5)	0.1 (0.0)	0.05 (0.0)	1.8 (1.0)
BGR2	14.5 (0.4)	7.0 (0.3)	9.0 (0.3)	39.1 (5.7)	19.2 (6.1)	2.4 (1.0)	45.7 (0.2)	0.3 (0.0)	0.05 (0.0)	3.4 (1.4)
NASA	15.6 (nd)	7.0 (nd)	3.0 (nd)	12.3 (nd)	319.3 (nd)	2.9 (nd)	124.5 (nd)	3.7 (nd)	0.25 (nd)	4.1 (nd)
NASH	18.3 (nd)	7.6 (nd)	4.1 (nd)	22.6 (nd)	18.2 (nd)	6.2 (nd)	28.5 (nd)	0.4 (nd)	0.04 (nd)	1.7 (nd)
Thaw lakes on mineral clays										
KWK1	17.1 (4.4)	6.1 (0.8)	9.2 (2.8)	39.0 (16.4)	14.1 (12.0)	2.2 (1.5)	36.8 (26.7)	0.3 (0.1)	0.05 (0.0)	8.0 (1.2)
KWK6	14.9 (0.8)	6.8 (0.4)	5.2 (0.0)	10.7 (0.7)	9.3 (1.1)	1.0 (0.4)	30.9 (3.0)	0.2 (0.0)	0.06 (0.0)	4.4 (1.6)
KWK12	16.8 (0.8)	8.0 (1.1)	8.6 (0.7)	39.6 (3.7)	13.8 (2.6)	1.6 (0.0)	27.7 (2.1)	0.2 (0.0)	0.08 (0.0)	2.5 (0.1)
KWK23	14.9 (0.2)	6.7 (0.2)	7.2 (0.6)	35.8 (1.9)	10.2 (1.9)	4.9 (0.6)	47.7 (5.6)	0.2 (0.0)	0.04 (0.0)	3.5 (1.9)
Thaw lakes on peatlands										
SAS1A	14.3 (0.2)	6.6 (0.3)	10.7 (0.8)	68.7 (2.7)	7.6 (2.6)	1.6 (0.3)	14.3 (0.9)	0.5 (0.1)	0.17 (0.0)	3.6 (1.2)
SAS1B	13.6 (0.1)	6.3 (0.3)	15.9 (0.4)	109.5 (3.9)	21.8 (5.4)	1.9 (0.4)	12.7 (2.2)	0.6 (0.1)	0.07 (0.0)	4.3 (0.1)
SAS2A	19.9 (nd)	6.2 (nd)	14.9 (nd)	98.4 (nd)	2.6 (nd)	3.1 (nd)	9.6 (nd)	0.7 (nd)	0.04 (nd)	1.2 (nd)
SAS2B	16.0 (nd)	6.0 (nd)	17.1 (nd)	116.9 (nd)	5.2 (nd)	1.3 (nd)	10.3 (nd)	0.5 (nd)	0.11 (nd)	0.9 (nd)
Shallow rocky basins										
SRB1	15.8 (2.2)	7.6 (0.6)	9.9 (0.0)	46.0 (6.5)	2.6 (1.2)	2.1 (0.6)	7.9 (2.8)	0.2 (0.1)	0.06 (0.0)	0.3 (0.1)
SRB2	13.8 (0.5)	7.6 (1.1)	13.2 (2.7)	68.8 (21.5)	1.3 (0.3)	1.4 (0.5)	11.2 (2.6)	0.2 (0.1)	0.14 (0.1)	1.4 (0.4)
SRB3	15.6 (0.2)	6.6 (0.2)	7.8 (1.4)	34.5 (9.5)	5.4 (2.0)	1.1 (0.1)	13.4 (2.8)	0.3 (0.1)	0.05 (0.0)	5.2 (0.6)
SRB4	15.0 (0.3)	7.9 (0.5)	10.4 (1.6)	20.0 (0.5)	5.0 (1.9)	0.8 (0.1)	5.7 (2.6)	0.8 (0.4)	0.44 (0.4)	2.4 (1.0)
SRB5	18.7 (1.8)	7.1 (0.9)	3.7 (0.1)	9.4 (2.7)	0.7 (0.1)	0.5 (0.2)	2.9 (1.3)	0.1 (0.0)	0.32 (0.2)	0.8 (0.0)

Table 2. The dominant photosynthetic and photoprotective accessory pigments (nmol L^{-1}), their sum (Σ) and ratio in the subarctic water bodies sampled in 2012.

Sites	Photosynthetic					Photoprotective							Ratio
	Allo	Chl b	Fuco	Perid	Σ	Cantha	Diadino	Echin	Lut	Viola	Zea	Σ	
Thaw lakes on marine clays													
BGR1	0.282	0.108	0.174	0.034	0.598	0.000	0.113	0.045	0.126	0.132	0.080	0.497	1.2
BGR2	0.053	0.159	0.611	0.343	1.167	0.073	0.483	0.088	0.372	0.442	0.677	2.134	0.5
NASA	2.078	0.401	0.101	0.000	2.580	0.000	0.000	0.000	0.745	0.308	0.000	1.053	2.4
NASH	0.161	0.204	0.740	0.000	1.106	0.184	0.464	0.208	0.208	0.568	1.692	3.324	0.3
Thaw lakes on mineral clays													
KWK1	0.641	1.681	0.702	0.458	3.481	0.147	3.836	0.202	1.435	0.847	0.375	6.843	0.5
KWK6	0.248	0.760	0.429	0.075	1.513	0.093	0.398	0.000	1.335	0.771	0.561	3.158	0.5
KWK12	0.290	0.202	0.569	0.151	1.213	0.046	0.358	0.089	0.337	0.354	0.111	1.295	0.9
KWK23	0.281	0.236	0.499	0.057	1.073	0.046	0.443	0.026	0.644	0.450	0.688	2.296	0.5
Thaw lakes on peatlands													
SAS1A	0.498	0.130	1.080	0.110	1.817	0.083	0.291	0.000	0.161	0.366	0.092	0.993	1.8
SAS1B	1.066	0.271	1.484	0.363	3.184	0.044	0.435	0.000	0.294	0.420	0.083	1.275	2.5
SAS2A	0.342	0.054	0.199	0.000	0.594	0.000	0.047	0.000	0.047	0.000	0.000	0.093	6.4
SAS2B	0.606	0.163	0.502	0.000	1.271	0.036	0.049	0.045	0.220	0.171	0.000	0.521	2.4
Shallow rock-basin lakes													
SRB1	0.018	0.038	0.051	0.017	0.124	0.000	0.026	0.008	0.045	0.069	0.026	0.175	0.7
SRB2	0.196	0.220	0.360	0.040	0.816	0.037	0.078	0.057	0.229	0.183	0.062	0.646	1.3
SRB3	1.026	0.352	2.011	0.261	3.650	0.103	0.460	0.219	0.557	0.924	0.530	2.792	1.3
SRB4	0.094	0.203	0.557	0.050	0.905	0.016	0.159	0.080	0.333	0.340	0.101	1.028	0.9
SRB5	0.066	0.048	0.420	0.004	0.537	0.010	0.085	0.031	0.064	0.199	0.087	0.477	1.1

Key: Allo, alloxanthin; Chl *b*, chlorophyll *b*; Fuco, fucoxathin; Perid, peridinin; Cantha, canthaxanthin; Diadino, diadinoxanthin; Echin, echinenone; Lut, lutein; Viola, violaxanthin; Zea, zeaxanthin.

Table 3. The relative concentration of bacteriochlorophyll *d* (BChl *d*, μg L^{-1}) based on the maximum peak area at 430 nm. The lakes have been arranged from lowest to highest concentrations.

Site	Date	Depth (m)	BChl *d* (μg L^{-1})
KWK6	4 Aug 2012	3.1	1.2
KWK6	21 Aug 2011	3.1	1.3
KWK23	4 Aug 2012	2.0	1.9
KWK12	3 Aug 2012	2.0	8.2
KWK12	19 Aug 2011	2.5	24.6
KWK1	19 Aug 2011	2.0	28.9
KWK23	4 Aug 2012	3.3	36.2
KWK23	21 Aug 2011	3.3	44.3
KWK1	3 Aug 2012	2.0	44.7
KWK12	3 Aug 2012	2.5	47.3

Table 4. RNA sequence analysis of eukaryotes in samples from permafrost thaw lake SAS2A, sampled in 2012. Each value is the % number of reads of the total for each sample (total number of reads minus rotifer sequences). The large fraction was retained on a 3 μm filter and the small fraction was on a 0.2 μm filter after filtration through the 3 μm pre-filter.

Taxonomic group	Percentage of reads			
	Surface		Bottom	
	Large	Small	Large	Small
Phytoplankton groups				
Dinophyta	17.11	4.02	8.71	1.90
Chrysophyta[a]	14.47	14.81	9.07	3.60
Chlorophyta[b]	9.97	2.03	2.11	0.40
Cryptophyta	3.10	1.71	2.39	0.65
Katablepharidophyta	2.71	1.00	0.11	0.20
Bacillariophyta	2.47	0.44	0.96	0.45
Raphidophyceae	0.51	0.33	0.00	0.04
Pavlovales	0.44	0.19	0.18	0.04
Prymnesiales	0.15	0.03	0.06	0.00
Other groups				
Ciliophora	22.94	43.55	62.95	83.90
Cercozoa	6.17	12.37	2.50	1.22
Fungi[c]	1.47	0.61	0.32	0.04
Centroheliozoa	1.44	0.80	0.11	0.12
Choanoflagellida	1.32	3.12	0.23	0.20
Perkinsea	0.00	0.00	0.03	0.12
Unknown affinities	15.75	15.00	10.28	7.11

[a]includes Chrysophyceae, Synurophyceae and Bicosoecida
[b]includes Chlorophyceae and Trebouxiophyceae
[c]includes Chytridiomycota, Oomycota and Ascomycota

Table 5. Closest identity (ID) of eukaryotic RNA sequences from permafrost thaw lake SAS2A to GenBank sequences (following a BLASTn search), at the lowest taxonomic level identified.

GenBank Taxonomy	Accession number	Isolation source	% ID	Percentage of reads	
				Surface	Bottom
Phytoplankton groups					
Chrysophyta					
Uroglena sp.	EU024983	FU44-26	99	6.03	0.03
Paraphysomonas sp.	JQ967316	Freshwater	99	0.67	3.78
Dinobryon divergens	KJ579346	WO33_4	99	0.40	0.00
Spumella-like flagellate	AY651098	Lake Mondsee	99	0.03	0.76
Cryptophyta					
Cryptomonas tetrapyrenoidosa	KF907407	Deokam032610	99	1.71	0.87
Cryptomonas pyrenoidifera	KF907397	CNUCRY 166	99	0.33	0.00
Cryptomonas curvata	KF907377	CNUCRY 90	99	0.06	0.28
Dinophyta					
Dinophyceae sp.	GQ423577	Lake Baikal	99	1.31	0.58
Peridinium wierzejskii	KF446619	Baikal region	99	1.03	2.07
Gyrodiniellum shiwhaense	FR720082	Shiwha Bay	98	0.49	0.01
Bacillariophyta					
Urosolenia eriensis	HQ912577	Y98-8	98	1.22	0.58
Chlorophyta					
Lemmermannia punctata	JQ356704	SAG 25.81	99	1.07	0.08
Chlorella sp.	Y12816	OvS/Ger1	99	1.00	0.00
Choricystis sp.	AY195972	AS-29	99	0.89	0.11
Koliella longiseta	HE610126	SAG 470-1	99	0.72	0.04
Monoraphidium sp.	KP017571	LB59	99	0.39	0.00
Raphidophyta					
Gonyostomum semen	KP200894	Freshwater	100	0.23	0.02
Prymnesiales					
Chrysochromulina parva	EU024987	FU44-40	100	0.09	0.03
Other groups					
Ciliophora					
Stokesia vernalis	HM030738	Freshwater	99	8.65	0.04
Cryptocaryon sp.	JF317699	Drinking water	99	0.89	5.61
Peniculida sp.	GQ330632	Peat bog water	98	0.83	1.85
Halteria sp.	GU067995	Lake water	99	0.49	6.38
Cyclidium marinum	JQ956553	Marine coast	99	0.00	34.42
Rhizaria					
Cercozoa	AB771834	Lake Kusaki	99	3.83	0.28
Fungi					
Saprolegnia sp.	FJ794911	Lake (parasite)	99	0.11	0.00
Penicillium brevicompactum	KP981369	ATCC 16024	99	0.00	0.10

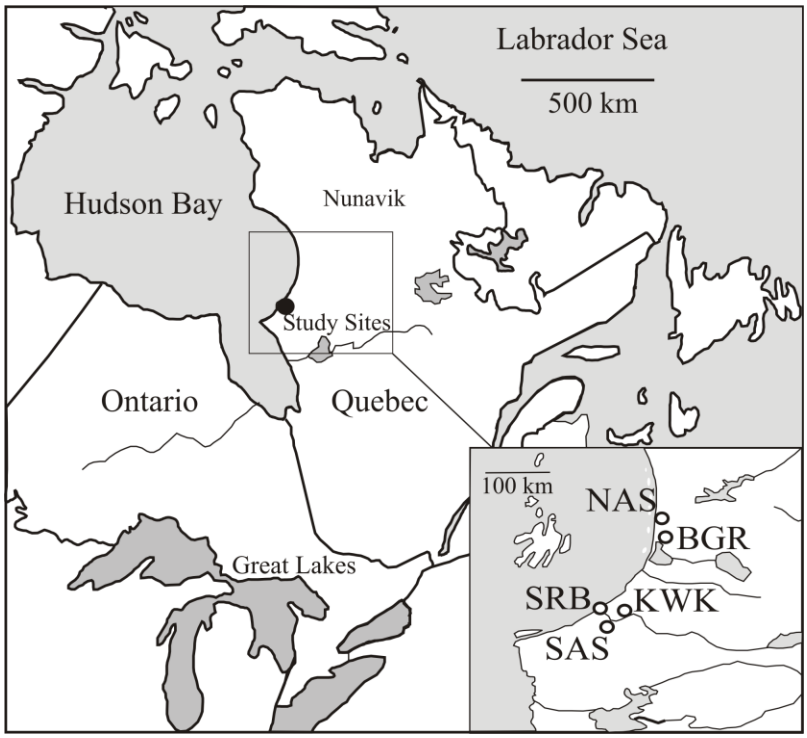

Figure 1. The location of the study area in Subarctic Quebec.

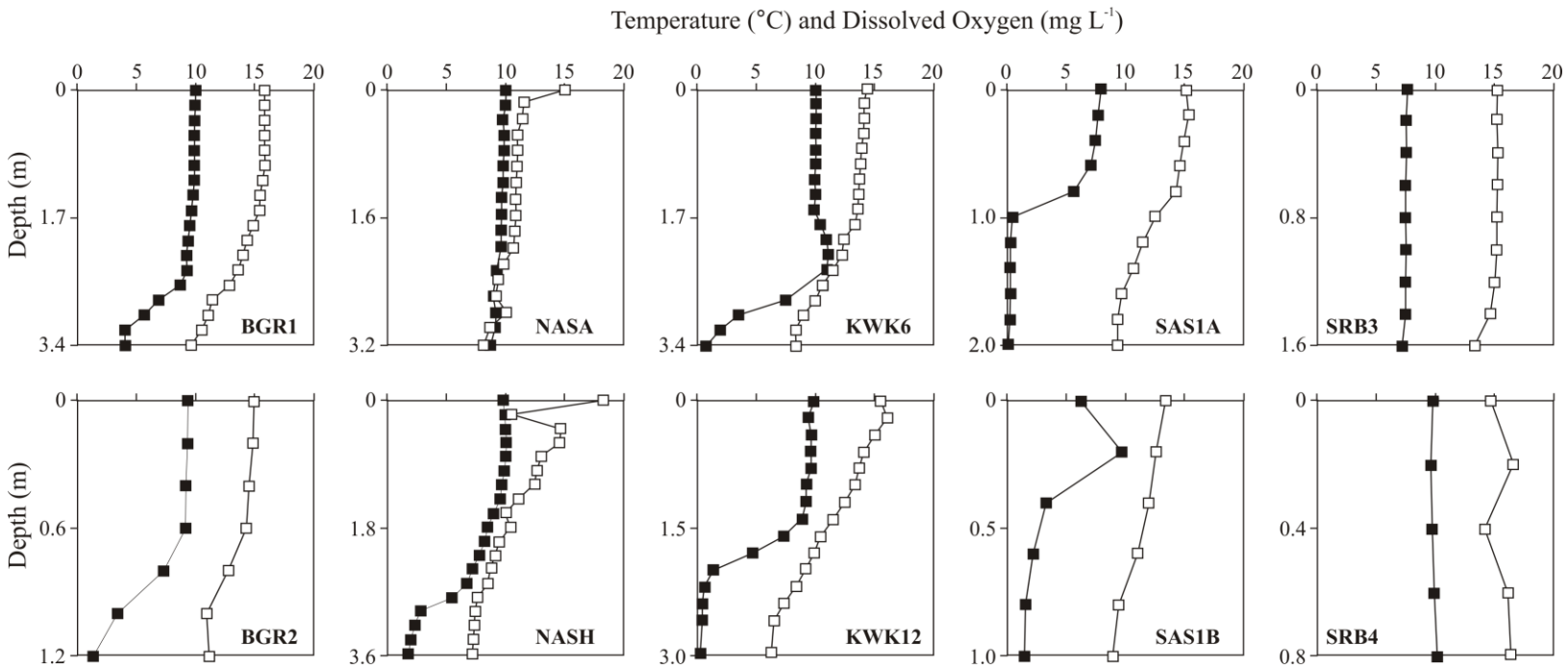

Figure 2. Temperature (white squares) and oxygen (black squares) stratification in permafrost thaw lakes (BGR, KWK, NAS, SAS) and shallow rock-basin lakes (SRB) during the summer 2012.

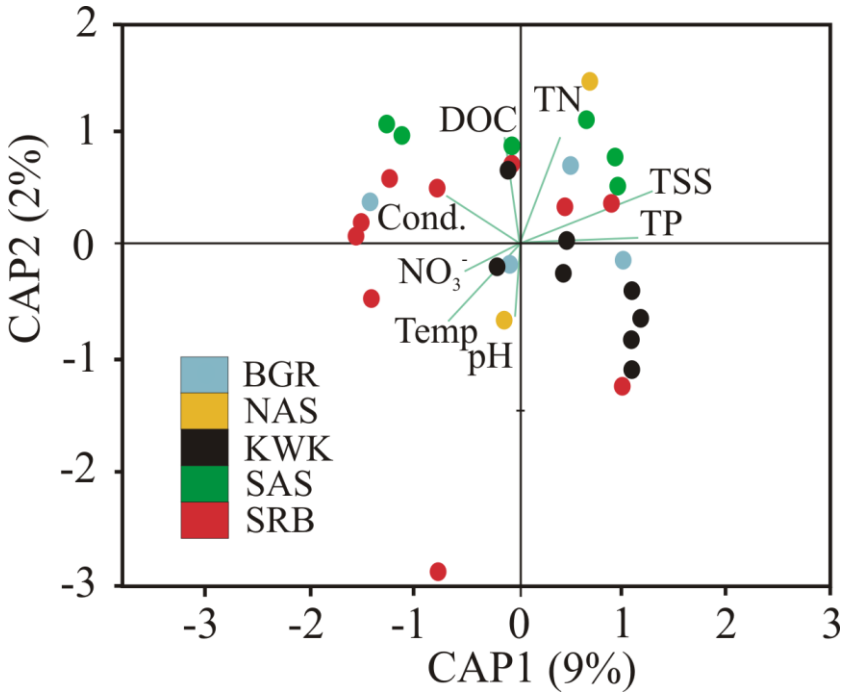

Figure 3. dbRDA of the pigment composition in the thaw and SRB lakes. Each circle represents individual lakes. The labelled lines represent the significant environmental vectors resulting from correlation analysis.

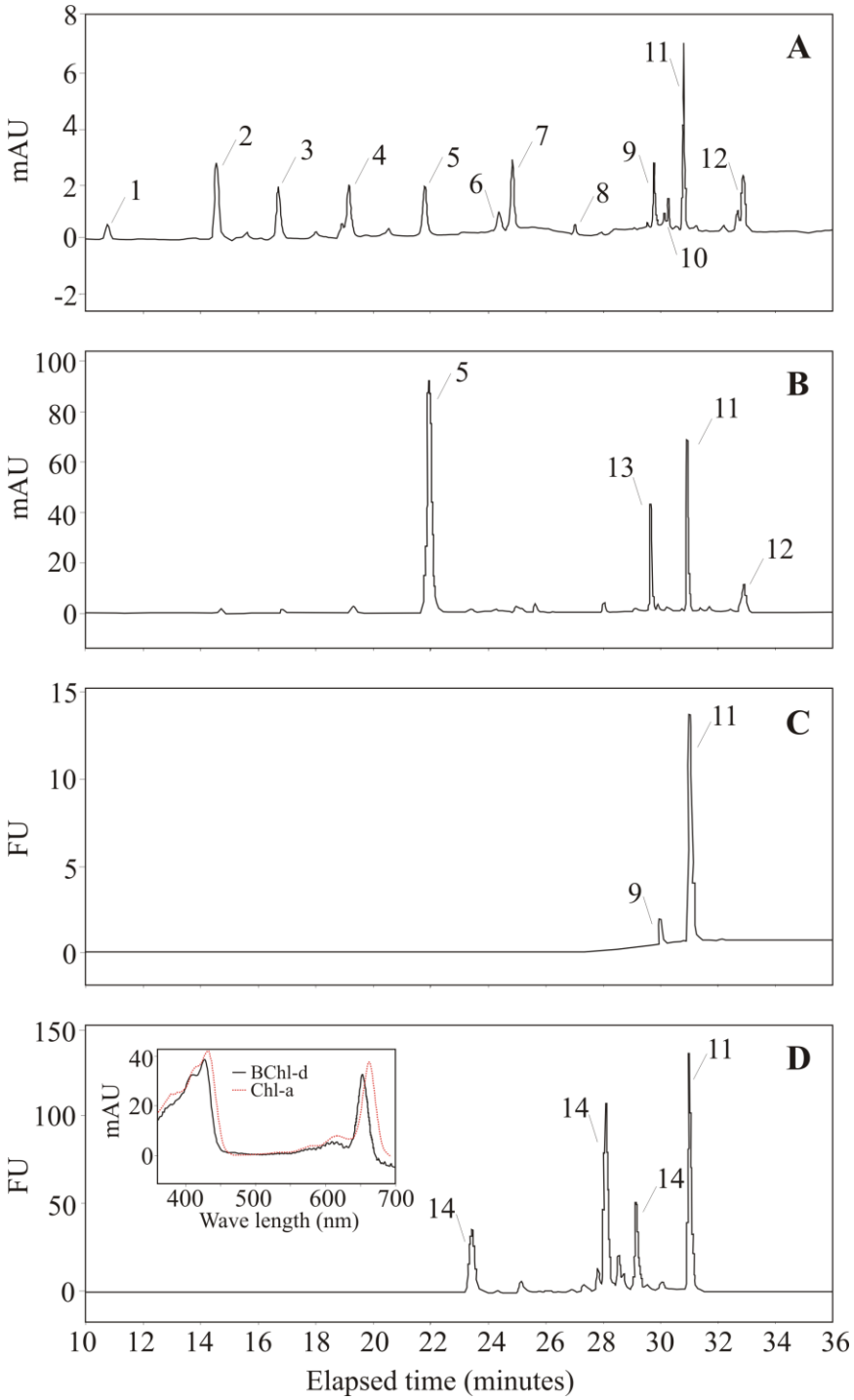

Figure 4. High-performance liquid chromatograms of lake KWK12 sampled on 3 August 2012: absorbance for the surface (A) or bottom (B) water layers and fluorescence for the surface (C) or bottom (D) water layers. Pigments from left to right: 1. Perid, 2. Fuco, 3. Viola, 4. Diadino, 5. Allo, 6. Zea, 7. Lut, 8. Cantha, 9. Chl *b*, 10. Echin, 11. Chl *a*, 12. β,β-Carotene, 13. Croco and 14. BChl *d*. Insert in panel D: Bacteriochlorophyll Chl *d* (BCHl *d*, black line) and Chl *a* (red line) absorption spectra (mAU = measured absorption units).

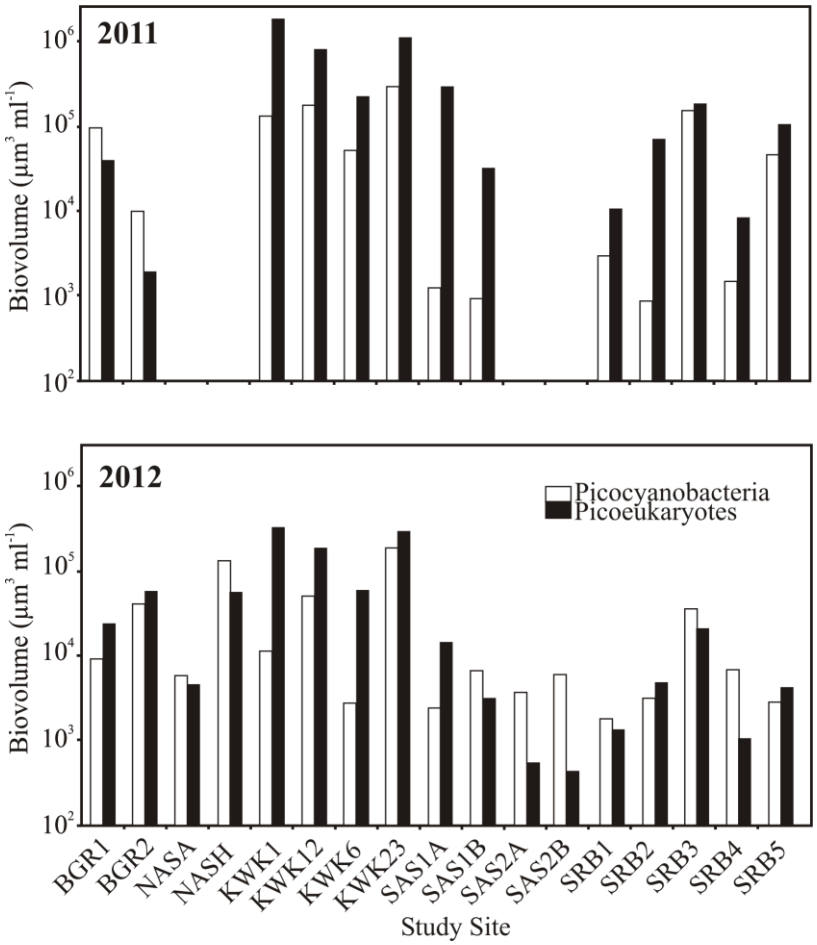

Figure 5. Picophytoplankton biovolume in the surface water of shallow rock-basin (SRB) and permafrost thaw lakes located on marine clays (KWK, BGR, NAS) and peatlands (SAS).

Supplementary material

Table S1. Location (latitude and longitude), maximum depth (Z) of the subarctic lakes and sampling dates. Water was sampled ca. 20 cm below the surface and ca. 20 cm above the maximum depth. The shallow rock basin lakes have been referred elsewhere as follows: WP1 (SRB1), WP2 (SRB2), Olsha (SRB3), 4 KM (SRB4), Iqalusiuvik (SRB5), – no sampling.

Sites	Latitude	Longitude	Z	Sampling dates	
			(m)	2011	2012
Thaw lakes on marine clays					
BGR1	56°36.650'N	76°12.900'W	3.5	20 Aug	9 Aug
BGR2	56°36.632'N	76°12.937'W	1.0	20 Aug	9 Aug
NASA	56°55.434'N	76°22.708'W	3.2	7 Aug	–
NASH	56°55.452'N	76°22.636'W	3.6	7 Aug	–
Thaw lakes on mineral clays					
KWK1	55°19.890'N	77°30.241'W	2.1	19 Aug	3 Aug
KWK6	55°19.937'N	77°30.117'W	3.2	21 Aug	4 Aug
KWK12	55°19.808'N	77°30.239'W	2.6	19 Aug	3 Aug
KWK23	55°19.947'N	77°30.131'W	3.4	21 Aug	4 Aug
Thaw lakes on peatlands					
SAS1A	55°13.128'N	77°42.477'W	1.9	23 Aug	5 Aug
SAS1B	55°13.143'N	77°42.475'W	1.7	23 Aug	5 Aug
SAS2A	55°13.591'N	77°41.815'W	2.6	–	13 Aug
SAS2B	55°13.600'N	77°41.806'W	2.0	–	13 Aug
Shallow rock-basin lakes					
SRB1	55°16.982'N	77°44.187'W	0.4	24 Aug	11 Aug
SRB2	55°16.970'N	77°44.122'W	0.8	24 Aug	11 Aug
SRB3	55°16.958'N	77°44.387'W	1.6	24 Aug	14 Aug
SRB4	55°19.907'N	77°41.959'W	0.7	16 Aug	8 Aug
SRB5	55°22.262'N	77°37.072'W	1.8	12 Aug	8 Aug